PHYSIQUE DE LA MATIÈRE EN GRAINS
PHYSICS OF GRANULAR MEDIA

The physics of fine powders: plugging and surface instabilities

Jacques Duran

LMDH – UMR 7603, CNRS–Université P. et M. Curie, 4, place Jussieu, 75252 Paris cedex 05, France

Abstract   The behavior of granular matter depends greatly on the size of its elementary components. Besides the well studied field of granulates made up of large sized particles which ignore the interaction of the particles with the fluid or gas environment, the physics of a collection of tiny particles such as fine or superfine powders concerns a majority of industrial applications. This paper briefly outlines several basic behavior of powders showing that new features come into play when the particle interaction with the surrounding gas is taken into account. It starts from two key mechanisms: the first arises when the typical particle velocity is in the order of the free fall velocity of that particle, which simply means that fluid drag comes into play. The second consists in considering the powder cakes as a porous material. Combining these two basic mechanisms with well-known granulate properties such as avalanching or heaping, leads to previously ignored sets of plugging effects or surface instabilities resulting from what we call the 'volcano effect'. Furthermore, we show that, up to a certain extent, the physics of fine powders interacting with gas, may mimic the physics of wetting liquids. *To cite this article: J. Duran, C. R. Physique 3 (2002) 217–227.*
© 2002 Académie des sciences/Éditions scientifiques et médicales Elsevier SAS

granular matter / powder / plugging / surface instability / volcano

Physique des poudres fines : bouchage et instabilités de surface

Résumé   Le comportement de la matière en grains dépend énormément de la taille de ses composants élémentaires. A coté du champ, déjà bien exploré, des milieux granulaires « secs » qui ignore l'interaction des particules avec les fluides environnants, la physique des collections de petites particules telles que les poudres fines et super-fines a été très peu explorée. Pourtant elle sous-tend une majorité d'applications industrielles. Cet article décrit briévement quelques uns des principaux comportements fondamentaux des poudres. Il s'intéresse à deux types de comportements fondamentaux. Le premier tient compte du fait que la vitesse caractéristique de chute libre des particules dans les gaz est du même ordre de grandeur que la vitesse d'entrainement, ce qui implique qu'il faille tenir compte des effets de freinage visqueux. Le second considère un empilement de particules comme un matériau poreux. En combinant ces deux effets avec les propriétés bien connus des milieux granulaires telles que les effets d'avalanche ou de mise en tas spontanée, on met en évidence des phénomènes de blocage et des instabilités de surface qui résultent de ce que nous appelons « l'effet volcan ». En outre, nous montrons que, dans une certaine mesure, la physique des poudres fines et sèches peut s'identifier à la physique des liquides mouillants.

E-mail address: jd@ccr.jussieu.fr (J. Duran).

217

DOSSIER

1. Basic equations and classification of powders

In a recent past, most of the theoretical, experimental and simulated works dealing with the physics of granular materials have considered collections of large solid particles (i.e. typically larger than 100 µm) or smaller particles under vacuum. This simplification allows us to neglect the complex interaction of the surrounding gases or fluids with the moving solid particles [1]. Except for the papers by Bocquet et al. [2] and Herrmann [3], all the papers in this publication start from this hypothesis. On the other hand, the dynamic behavior of fine powders [4–9] interacting with gases (fluidized beds) or liquids [10,11] is recognized as the keystone of a large number of technological processes, e.g. in fine chemicals and pharmaceuticals, ceramics and food industry. In nature, huge fields of well known patterns such as dunes [3,12] and ripples result from sand–wind interaction in deserts or sand–water interaction on sea shores.

In the following, we first remind the reader of a few basic equations dealing with fluid–particle interactions and we derive a classification among different species of granular materials which is akin to the classification first put forth by Brown and Richards [13] in the 1970s. Next we consider the classical situation of plugging during a duct flow which is often met in industrial environment. We show that the value of the angle of repose of a fine powder is markedly increased when the powder is submitted to gas or air blow, thereby largely increasing the probability of building up unwanted plugs. The last part of the paper is devoted to the observation and models of the various kinds of instabilities obtained when blowing a fine powder from below. We explain that several issues of the physics of fine powders (or of larger particles in liquids such as slurries), up to some extent, show similarities with the physics of wetting liquids. We suggest the potential extrapolation of this work to geological situations.

Under normal conditions the kinetic and potential energies of large particles such as desert sands (100 µm diameter) are so large that these particles would become Brownian at a preposterous temperature. In reverse, we can estimate the diameter D of a solid particle which could be Brownian at room temperature. We set $kT \approx mgD \approx \frac{1}{2}mv^2$, where m is the particle mass, g the gravitational acceleration and v a realistic velocity (say 1 cm·s^{-1}). We find that Brownian motion and thus temperature cannot be ignored in the case of particles whose size is smaller than 1 µm. These set of tiny particles are commonly called 'fumes'. They are known to have infinite or very large deposit times.

First, we build up a significant number $\Re$ (which is equivalent to the familiar Reynolds number in hydrodynamics) which measures the ratio between the particle energy and the energy loss by laminar and turbulent drag in a fluid [14]. In the case of laminar drag around a sphere, we get

$$\Re_l = \frac{1}{36}\frac{\rho_b}{\eta}Dv,$$

and in the case of turbulent drag

$$\Re_t \approx \frac{1}{0.24}\frac{\rho_b}{\rho_0},$$

where ρ_b is the particle density, η and ρ_0 the fluid viscosity and density. Numerical estimates show that particle–fluid interaction should be taken into account ($\Re \lesssim 1$) when particle size is of the order of 10 µm.

Table 1. Classification of granular materials with respect to particle–fluid interaction

Generic	Name	Size (μm)	Interaction
Powder	Ultra-fine	0.1–1.0	Temp. and gas
Powder	Super-fine	1–10	Gas
Powder	Granular	10–100	Liquids
Granular solids		100–3000	Viscous fluids
Broken solids		> 3000	Viscous fluids

Moreover, we note that due to laminar drag, the free fall velocity v_{ff} (when the particle weight balances the Stokes force) of a solid sphere is given by

$$v_{ff} = \frac{D^2}{18\eta}\rho g. \tag{1}$$

As an example the free fall velocity of a glass sphere ($R = 10$ μm) is about 25 mm·s^{-1} which is just the same value as for a 100 μm solid particle falling in water or for a 10 cm large solid rock moving in a liquid lava or viscous palehoe lava. From this viewpoint, some features of the physics of super fine powders in air, up to a certain extent, can mimic the behavior of granular particles in liquids as well as of rocks in hot lava and thus may deal with geological concerns. Using these simple arguments, we can build up a classification of powders and various granular materials as reported in Table 1 which is an extension of the previously reported classification first put forth by Brown and Richards [13] in the 1970s.

Secondly, we observe that the compacted form of a powder can act as a porous solid material with respect to a fluid flow. In the case of a poiseuille (i.e. laminar which means relatively slow) flow, the velocity of the fluid emerging from a powder cake whose thickness is L, is given by the Darcy equation

$$v = \frac{K}{\eta}\frac{\Delta P}{L}, \tag{2}$$

where ΔP is the difference of pressure between both ends of the cake and K is the permeability of the powder which is on the order of magnitude of the pores area.

2. Plugging: the angle of repose of blown powders

Firstly, we examine the problem of a compacted fine powder submitted to an air blow which is forced through the granular medium. This situation is commonly met in pharmaceutical or chemical industry, e.g. in air activated powder ducts. Since frequent plugging happens in powder ducts, engineers tried to overcome these problems using blown air. Unfortunately and as we show in the following, even a very slight air blow, at a very small velocity turns out to steepen the angle of avalanche of the powders, eventually leading to plugging and counterproductive results.

In order to analyse experimentally the steepening mechanism of the avalanche angle due to gas blow, we set up the experiment sketched in the left-hand side of Fig. 1. The cylindric container (about 1 m long and 5 cm in diameter) partially filled with a dry powder, can be inclined at any angle θ with respect to horizontal. The experiment consists in imputing a given gas (nitrogen or helium) at a flow rate Q which results in a measured pressure difference ΔP between both ends of the tube. The tube is rotated around an axis perpendicular to the figure plane and the maximum avalanche angle is optically measured using an external device. Series of typical experimental results are reported in the right-hand side part of Fig. 1.
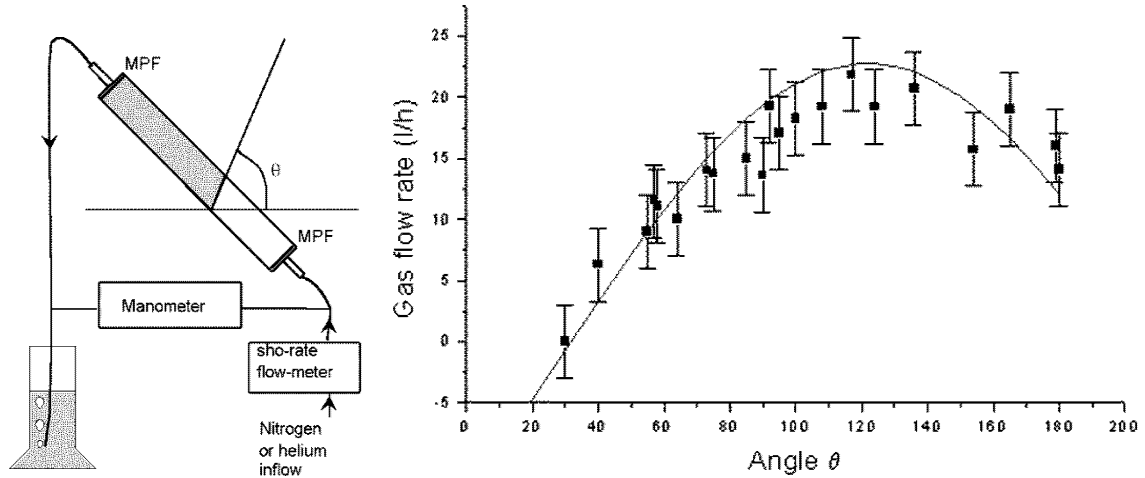
Figure 1. Left: the experimental setup: the monitored gas laminar flow goes through the fine powder contained in the inclined leucite tube whose two ends are closed by two micro-pore filters. The pressure difference between gas input and output is also monitored. MPF are micropore filters. Right: the experimental results: the dark line corresponds to theory. The square dots are experimental results obtained with nitrogen and light hollow plastic spheres (diameter 25 μm).

These experimental results show that the avalanche angle is quite sensitive to air blow. For example, a very slow gas velocity as small as 3 mm·s^{-1} is able to stabilize the avalanche angle up to 180°, which means that the powder flow can be fully stopped even in a reverted vertical tube.

The basic equations for this situation can be expressed as follows. Consider a granular material sitting at avalanche angle θ to the horizontal. The tangential force [16] needed to have the avalanche slide down at θ is $T = P \sin\theta = \mu N$ where P is the weight of the superficial slice of material. Blowing an air flow perpendicular to the surface, we add a normal force $F(v)$. The total normal applied force is $N = P\cos\theta + F(v)$. Since an avalanche happens when $\tan\theta = \mu$, the balance becomes:

$$F(v) = \frac{P(\sin\theta - \mu\cos\theta)}{\mu}. \tag{3}$$

Actually, the quantitative solution to this problem is far from being straigthforward because the externally applied normal force due to the air flow is not equivalent to simply adding a superficial weight to the sliding sheet. Experiments will determine how the problem should be handled.

We start from a real example and we consider the limiting case when the tube is vertical and the powder material is kept from falling down using a slow vertical air flow coming from below ($\theta = 180°$). Using a set of spherical hollow powder particles (mean diameter 35 μm) we find that an air velocity of 2.64 mm·s^{-1} is able to prevent the powder from falling down. Calculating the free fall velocity v_{ff} of each of these particles, we find $v_{ff} \simeq 14$ mm·s^{-1} which is 6 times more. This means that the powder should be considered as a whole in this problem rather than as isolated particles even in this particular situation. Using the measured pressure difference between the two ends of the powder cake (11.4 mbars), we calculate the force acting over the superficial slice of material due to the pressure difference between both sides of this particular slice, assuming a linear pressure distribution (poiseuille flow through the porous cake). We find that this force is about $3.2 \cdot 10^{-4}$ N which, within a good approximation, equals the weight of a single monolayered slice of powder. In brief, this result shows that the problem of the steepening of the avalanche angle by a gas flow should be handled by considering the powder cake as a stacking of separated sheets of granular

material, each one undergoing a part of the total pressure. Using this consideration and Eq. (3), we were able to satisfactorily fit the experimental results reported in Fig. 1.

A useful remark from the practial viewpoint, is compulsory: a very slight gas flux going through a powder cake is able to steepen markedly the avalanche angle. It ensues that care should be taken when attempting to favorize powder flows in ducts or pipes using air blow as is commonly done in industry. Instead of using a laminar and parallel gas flow, it should be much more efficient to use convective or non-evenly distributed (possibly chaotic) air flux in order to prevent the steepening effect we have just mentionned above.

2.1. Thick-layer surface instability

Our present knowledge about instability of horizontal layers of granular solids (i.e. large particles) under vertical vibrations is currently firmly established [9,17–20]. On the other hand, the vibrational heaping of a sand pile has motivated a lively debate [21–23] dealing with the influence of air [1] in the phenomenology of sand heaping.

In reverse, basic features of the surface instability of tapped fine powder layers are yet unknown. They can be readily observed starting from a simple table-top experiment which duplicates into a small scale laboratory experiment, a real industrial device used to empty powder carrying tankers: we use a cylindrical transparent tube made of leucite or glass. We half fill the tube with fine dry powder (e.g. glass beads, diameter 20 μm). We keep the tube horizontal and rigidly fixed at both ends, with the powder initially set flat and horizontal thus giving a granulate thickness of about 10 mm in the center. We knock gently and repeatedly at a very low frequency and at a constant intensity onto the center of the tube from below, applying vertically as brief taps as possible. After a few taps (about ten to twenty), the surface, initially flat, smooth and horizontal, turns out to exhibit ripples similar to those reported in Fig. 2, (a) and (b). Tapping 'more energetically' but still keeping the intensity as constant as possible from one tap to the next, induces a pattern where the mean distance between two successive ripples increase significantly. Furthermore and under energetic tapping, a careful observation of the surface shows that, at every tap, a limited number of particles may be ejected upwards starting both from the apices of the hills and from the small plateaux which happen occasionally between imperfectly joined hills.

More reliable information has been obtained in the course of our experiments, using a CCD (charge coupled device) camera above the tube in order to record and process the successive patterns. We used
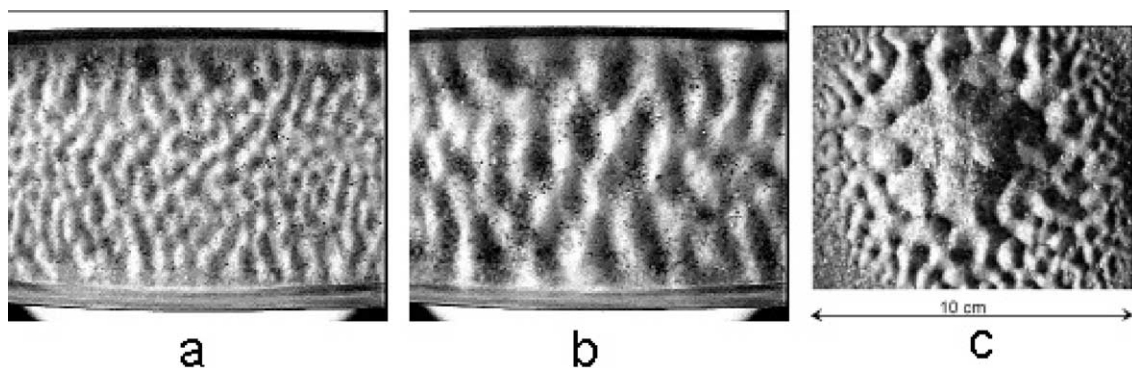

Figure 2. Three bird's-eye views of the corrugated surface observed after twenty shocks of constant amplitude onto the underpart of the containers. Snapshots (a) and (b) corresponds to the cylindrical container and are obtained at two different shock amplitudes, larger in (b) than in (a). Measurements are performed in the median part of the pattern. Snapshot (c) is obtained in a rectangular metallic box (size 20×40 cm^2) containing a layer of fine beach sand, tapped under the central part. In this latter case, the pattern reproduces the transient deformation of the underlying metallic sheet.
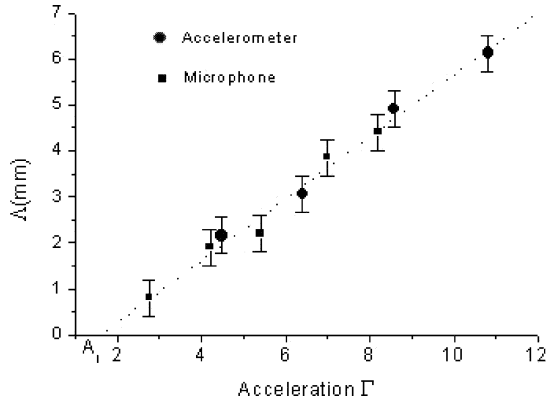
Figure 3. Characteristic wavelength of the pattern in millimeter versus taps amplitude measured as the signal delivered by the microphone in tens of millivolts. The dotted line shows the linear fit of the experimental results according to the theoretical model.

a magnetically driven tapping device and a microphone or an accelerometer stuck on the tube in order to monitor the amplitude of the taps applied on the sample. Typical experimental results are reported in Fig. 3.

First, it is observed that, after a few taps, the surface displays a regularly corrugated pattern made of a succession of joined heaps sitting at the natural avalanche angle. The crucial point here is that any further taps do not induce any significant change in the pattern which thus can be considered as a steady state with respect to further vertical shocks. Second, and this is a clue to the understanding of the process, the characteristic wavelength of the pattern is found to be directly proportional to the amplitude of the taps.

We call h_T the altitude (starting from the bottom of the container) of the apices of the corrugated surface, h_B the altitude of the valleys of the corrugated surface and h_i the altitude of the initially horizontal surface of the granular layer. θ is the avalanche angle of the powder, which is about 30° for our glass beads powder. The wavelength Λ is given by $\Lambda = 2(h_T - h_B) \cot \theta$ where $h_T + h_B = 2h_i$. Starting from Eq. (2), we see that ΔP is proportional to the tap amplitude A applied on the underpart of the tube so that the velocity v_h of the air emerging from the surface at altitude h can be written as $v_h = \alpha A / h$ where α is the coefficient of proportionality given by Darcy's law which involves the permeability of the granular material.

We realize that the air slowing down process through the granular layer is unable alone to account for the observations described above. If we imagine that the incoming air pulse is unable to eject particles when reaching the apices of the hills, we have $\alpha A_T < h_T v_f$. Calculating the ratio of the required initial velocity to induce hills of height h_T to the required initial velocity for the onset of the corrugation, we get $A_T / A_{ic} = h_T / h_i$. Our experiments show that the ratio h_T / h_i is only marginally larger than 1 while the observed amplitude ratio is about 8 (Fig. 3). Thus, another process should be taken into account to explain the observed features.

On both sides of the hills, the ascending air flux meets an inclined sheet of particles which is on the verge of avalanching. Under these circumstances, one particle subjected to the vertical incoming air flux bears a fraction of the additional weight of the above lying particles involved in the avalanche layer (see insert in Fig. 4).

This additional mass opposes the blowing up of the particles near the surface and therefore stabilizes the inclined lateral surfaces against the incoming air flow. We can build up a simplified equation for this screening effect considering that the mass of the concerned particle is increased by a factor $Np \sin \theta$, N being the number of the particles lying above pertaining to a single sheet of the inclined granulate and p being the unknown number of sheets possibly involved in the avalanche process. Strictly speaking these particles participating to the screening effect need not move, i.e. fall in an avalanche process. Considering that all the particles pertaining to the superficial sheet and sitting above the considered particle sitting at altitude h participate to the screening effect, we have $Np \simeq (h_T - h)p/D$. The air velocity required, v_{ah}, to eject the considered particle sitting at altitude h is given by $v_{ah} = v_f(h_T - h)p \sin \theta / D$. This screening effect determines a cut-off altitude h_C under which all the particles sitting on the inclined lateral surface
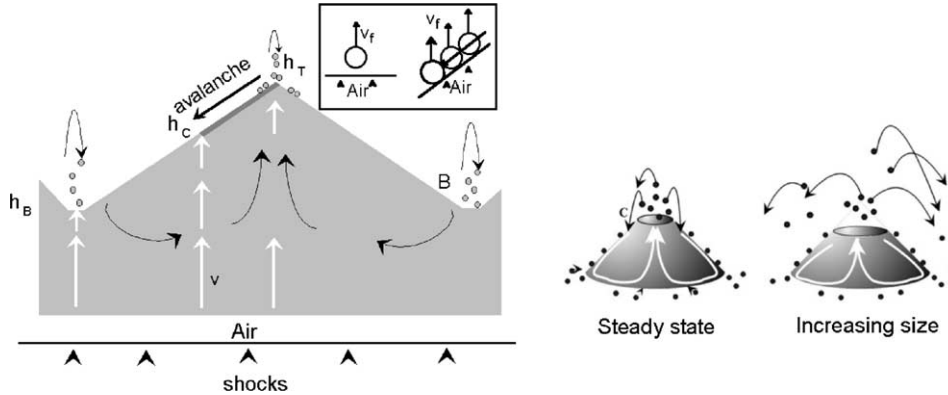
Figure 4. Left: sketch of the ripples buildup showing the screening effect of the inclined sides of the hills with respect to air blown from below. The white arrows correspond to air trajectory while the black ones show the movement of the particles. Insert: the balance of forces on a horizontal and on an inclined surface. Right: sketch of the trajectories of the powder particles participating to the intrinsic convection process when the heap are ejected above the plate resulting from either taps or air blowing from below.

cannot be expelled by the air flux. This altitude h_C is given by the equation:

$$\alpha \frac{A - A_i}{h v_f} \frac{1}{\frac{h_T - h_C}{D} p \sin\theta} \simeq 1. \tag{4}$$

In brief, the upper part of the hill (when $h_C < h < h_T$) is unstable whereas the lowest one (when $h_B < h < h_C$) is stable against vertical air blown from below. We note that the steady state of the pattern should result from the balance between the small number of expelled particles near the apices and the number of particles which are re-injected into the bulk of the hills at every tap (see black arrows in Fig. 3). We conjecture that this sort of trapping-detrapping process should be independent of the size of the hills. We write $h_T - h_C = C(h_T - h_B)$ where C is the proportion of the unstable part of the hills. It is a dimensionless constant independent of the height of the hills and of the amplitude of the shocks. With this extra assumption, we get the characteristic wavelength Λ of the pattern which is proportional to the amplitude of the shocks in agreement with the measurements reported in Fig. 2:

$$\Lambda \simeq 2 \frac{\alpha}{C} \frac{A - A_i}{h v_f} \frac{D}{p \sin\theta} \cot\theta. \tag{5}$$

We find that $C = 25\%$ of the hills are unstable if only one single layer of powder is involved in the process. If, now, five layers of the superficial sheet participate to the process as has been repeatedly observed in avalanche experiments, we see that only 5% of the upper part of the hills are unstable against the incoming air flux.

The delicate question of the stability of the particles sitting near the apices of the pattern has motivated a further experiment which we performed firstly in order to prove directly the validity of our model based on air–powder interaction and secondly to provide a visual insight into the question of the stability of the apices of the air built pattern.

We use a millipore filter, commonly used in chemistry for filtering, in a reverse manner. A plastic filter (pores 3 μm) is placed at the bottom of a commercial cylindrical glass vessel which allows direct observation or image processing with a CCD camera. In contact with the horizontal filter and above it, we lay a thin layer of powder (about 8 mm thick). Instead of sucking up through the filter as is usually done, we blow from below, using either brief air pulses or a continuous air flux.
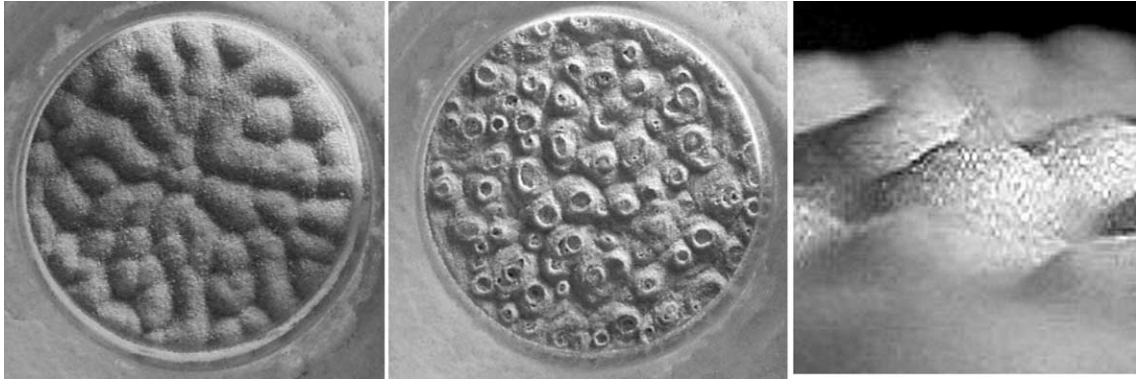
Figure 5. The left photograph show the ripples obtained by using fast transient air pulses. The middle photograph is obtained with a continuous air flow exhibiting small craters (black points) sitting at the center of the myriads of small fixed volcanoes. At right, an instantaneous close lateral view of eruptive micro volcanoes. The volcano effect is clearly seen. The photograph scale is about 5 cm for the two left snapshot and about 3 mm for the right one.

The photographs of the resulting surface corrugation are reported in Fig. 5. The left snapshot shows up a surface corrugation made up of triangular shaped ripples quite similar to the previously reported in our tapping experiments (Fig. 2). The center snapshot corresponding to a gentle and continuous air flow going through the powder cake is quite informative. Then the surface corrugation exhibits a different aspect because the system has no time to relax between separate successive perturbations as in the preceding experiments. As expected from the preceding consideration this experiment shows up a myriad of stable small volcanoes organized around small craters (seen as black spots in the snapshot) which spew out powder particles (right-hand side snapshot).

2.2. Thin film instability: analogy with wetting liquids

Keeping along this line, we take a further step, considering now a thin slice (typically a monolayer) of a fine powder spread out over a flat plate. Again, we knock gently and repeatedly at a very low pace and at a constant intensity over one corner of the glass plate, applying vertically as brief taps as possible. After a few taps (about ten to forty), the surface, initially flat, smooth and horizontal, separates into a collection of tiny rounded conical heaps looking like droplets similar to those reported in Fig. 6. Starting from the same initial conditions but tapping more energetically while keeping the intensity as constant as possible from one tap to the next, induces a pattern with bigger droplets separated by a larger distance. The resulting patterns strikingly remind one of the Rayleigh–Taylor instability illustrated by the droplets structure obtained when turning up a glass plate initially covered with a thin film of a wetting liquid. As we will show in the following, this analogy is not fortuitous. It results from an underlying similarity between the equations governing the wetting properties of liquids and the behavior of powder piles interacting with a surrounding gas.

Using the same experimental setup as above, we get series of experimental results as reported in Fig. 7. Consider the initial situation when a thin slice of powder of thickness e made of small spherical beads (diameter D) is evenly spread over a horizontal flat surface whose area is S. Suppose that the powder has been gathered in a number of N disjoint identical conical piles having an angle θ to the horizontal and culminating at altitude h. These piles are evenly distributed over the area S. The wavelength Λ of this pattern is the square root of the mean area occupied by each pile:

$$\Lambda = \sqrt{\frac{\pi}{3e\tan^2\theta}} h^{\frac{3}{2}} \propto h^{\frac{3}{2}}. \tag{6}$$
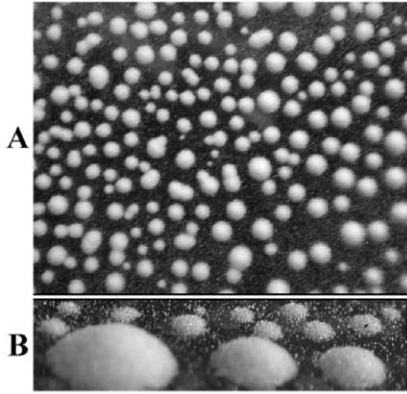
Figure 6. Above: bird's eye view of the pattern obtained after fourty taps over a plate initially covered with an approximately uniform film of powder particles (diameter about 30 μm). The mean distance between neighbouring heaps is about 5mm. Below: the snapshot shows an oblique view of a few small heaps. It exhibits the rounded shape of the apices due to the 'volcano effect'.
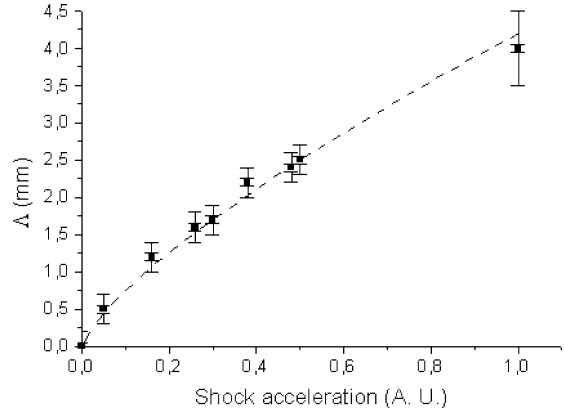

Figure 7. Experimental results obtained with a monolayer slice of silica powder (particle size about 35 μm). The dashed line is a theoretical best fit to Eq. (6).

Starting from the same consideration as above, giving Eq. (4), the basic equation governing the problem becomes:

$$\frac{K\Delta P}{Dh_C} = \rho\left(\frac{1}{18}\frac{C}{1-C}p\sin\theta\right)gh_C. \tag{7}$$

Written in this form, it can be seen as describing the balance between two antagonistic pressures:

- A 'hydrostatic' pressure $P_g = \rho^*gh_C$ which accounts for the screening effect of the avalanche properties of the powder, where

$$\rho^* = \rho\left(\frac{1}{18}\frac{C}{1-C}p\sin\theta\right)$$

 is the normalized density of the particles sitting near the apices and participating to the avalanches.

- The equivalent of a Laplace–Young pressure, P_l (describing the pressure difference at the interface of two liquids) which can be written

$$P_l = \frac{K\Delta P}{Dh_C} = \gamma^*\left(\frac{2}{h_C}\right), \tag{8}$$

where γ^* plays the role of a surface tension and is defined by $\gamma^* = K\Delta P/(2D)$.

Equation (7) describes the equilibrium of the analogue of a wetting liquid droplet [24] on an horizontal plate. We mimic a conical powder pile with a half spherical wetting material of height h_C and curvature $2/h_C$ and surface tension γ^*. This analogue to a surface tension can be seen as resulting from the convective forces (Fig. 1) which drag powder particles from the surrounding surface and subsequently inject them into the powder pile. It has a purely dynamic origin and results from the convective forces related to the volcano effect. From Eq. (7), we get the cut-off length h_C from the following relationship:

$$h_C \simeq \left(\frac{K\Delta P}{D}\frac{1}{\rho^*g}\right)^{\frac{1}{2}} = \left(\frac{2\gamma^*}{\rho^*g}\right)^{\frac{1}{2}}. \tag{9}$$

225

Table 2. Basic equations for a wetting liquid and a blown powder

Wetting liquid	Equation	Blown powder heap	Equation
Surface tension	$\gamma = \dfrac{dF}{dl}$	Convective forces	$\gamma^* = \dfrac{K\Delta P}{2D}$
Droplet radius	R	Heap height	h_C
Laplace–Young law	$\Delta P = \dfrac{2\gamma}{R}$	Eq. (8)	$\Delta P^* = \dfrac{2\gamma^*}{h_C}$
Droplet equilibrium	$\dfrac{2\gamma}{R} = \rho g R$	Blown heap equilibrium	$\dfrac{2\gamma^*}{h_C} = \rho^* g h_C$

Going on with the analogy to wetting liquids [24], we can also define the usual capillary length λ equating the hydrostatic pressure and the Laplace–Young pressure so that $\lambda = (\gamma^*/\rho^* g)^{1/2} = h_C/\sqrt{2}$ and a related Bond number $Bo = (\rho^* g h_C^2/\gamma^*)$.

Using Eq. (6), we find

$$\Lambda = \sqrt{\frac{\pi}{3e\tan^2\theta}}\left(\frac{K\Delta P}{D}\frac{1}{\rho^* g}\right)^{\frac{3}{4}} = \sqrt{\frac{\pi}{3e\tan^2\theta}}\left(\frac{2\gamma^*}{\rho^* g}\right)^{\frac{3}{4}}. \tag{10}$$

We calculate an approximate value for the surface tension γ^* starting from Eq. (10) using typical values for Λ (5 mm), e (20 μm) and ρ^* obtained for $C = 5\%$. We get $\gamma^* \simeq 2.3 \cdot 10^{-5}$ N·m^{-1} which means that this constant is about 3000 times smaller than the surface tension of pure water. As expected, λ and h_C are in the order of 1 mm. Moreover, starting from Eq. (8) we can get an estimated value for the pressure difference between the altitude h_C and the base. We consider that the permeability of the granular material is a fraction of the cross sectional area of a single particle. Thus, we get ΔP in the order of 3 Pa. This quantity should be a fraction of the maximum possible air pressure due to the total weight of the powder pile leaning on the basis surface S. This maximum air pressure is found to be about 10 Pa which therefore stands as a correct order of magnitude. Table 2 sketches the analogy between the basic equations governing the powder heap equilibrium and the equations governing the equilibrium of liquid droplets.

Starting from this analogy and using, e.g., Eq. (7), we can transcribe the classical demonstration of the Rayleigh–Taylor instability for wetting liquids. The standard analysis consists in examining the evolution of an infinitesimal sinusoidal distortion of the initially flat surface. Note that the basic calculation for liquids (found in text-books) leads to a wavelength dependence $\Lambda \propto (\gamma/\rho g)^{1/2}$. Here, the distortion is by no means infinitesimal. We rather introduced the volume conservation condition which leads to $\Lambda \propto (\gamma^*/\rho^* g)^{3/4}$. But except for this difference, the underlying phenomenology of the blown powder mimics the standard Rayleigh–Taylor instability. A series of further experiments can be found at the URL: www.espci.fr/DirectionJD/.

Even if it has the merit of establishing a connection between the (yet unknown) description of blown powder properties and the (already known) wetting liquids behavior, our simple theoretical explanation certainly lays itself open to several criticisms. Note that this theoretical model may also well apply to the situation of vibrated granular slurries in water [26] and maybe extrapolate to larger natural situation involving real volcanoes fields and other landscapes. Note that it does not convey any information regarding the development of the surface instability. Such an analysis would involve the introduction of a sort of powder viscosity [25] which is not considered in the present model dealing with the steady state of the process. A time resolved scrutiny of the pattern growth would probably convey information about this question.

References

[1] H.K. Pak, E. Van Doorn, R.P. Behringer, Phys. Rev. Lett. 74 (1995) 4643–4646.

[2] L. Bocquet, E. Charlaix, F. Restagno, C. R. Physique 3 (2) (2002) 207–215.

[3] H.J. Herrmann, C. R. Physique 3 (2) (2002) 197–206.

[4] T. Raafat, J.P. Hulin, H.J. Herrmann, Phys. Rev. E 53 (1996) 4345.

[5] A. Castellanos, J.M. Valverde, A.T. Perez, A. Ramos, P.K. Watson, Phys. Rev. Lett. 82 (1999) 1156.

[6] E. Falcon, K. Krumar, K.M.S. Bajaj, J.K. Bhattacharjee, Phys. Rev. E 59 (1999) 5716.

[7] C. Laroche, S. Douady, S. Fauve, J. Phys. 50 (1989) 699–706.

[8] J. Duran, Phys. Rev. Lett. 84 (2000) 5126.

[9] L.S. Tsimring, R. Ramaswamy, P. Sherman, Phys. Rev. E 60 (1999) 7126–7130.

[10] J.M. Valverde, A. Castellanos, M.A. Sanchez Quintilla, Phys. Rev. Lett. 86 (2001) 3020.

[11] R.D. Wildman, J.M. Huntley, D.J. Parker, Phys. Rev. Lett. 86 (2001) 3304.

[12] K. Kroy, G. Sauermann, H.J. Herrrmann, cond-mat/0101380.

[13] R.L. Brown, J.C. Richards, Principles of Powder Mechanics, Pergamon Press, Oxford, 1970.

[14] J. Duran, Sands, Powders and Grains, Springer, New York, 2000.

[15] C.A. Coulomb, Mem. Math. Acad. R. Sci. 7 (1776) 343.

[16] R.M. Nedderman, Statics and Kinematics of Granular Materials, Cambridge Univ. Press, Cambridge, 1972.

[17] F. Melo, P.B. Umbanhowar, H.L. Swinney, Phys. Rev. Lett. 72 (1994) 172.

[18] P.B. Umbanhowar, F. Melo, H.L. Swinney, Nature 382 (1996) 793.

[19] F. Melo, P.B. Umbanhowar, H.L. Swinney, Phys. Rev. Lett. 75 (1995) 3838.

[20] E. Clément, L. Vanel, J. Rajchenbach, J. Duran, Phys Rev. E 53 (1996) 2972.

[21] S. Fauve, S. Douady, C. Laroche, J. Phys. C 3 50 (1989) 187.

[22] P. Evesque, J. Rajchenbach, Phys. Rev. Lett. 62 (1989) 44.

[23] E. Clément, J. Duran, J. Rajchenbach, Phys. Rev. Lett. 69 (1992) 1189.

[24] P.-G. de Gennes, Rev. Mod. Phys. 57 (1985) 827–861.

[25] S.T. Thoroddsen, Q. Shen Amy, Phys. Fluids 13 (2001) 4–6.

[26] J. Schleier-Smith, H.A. Stone, Phys. Rev. Lett. 86 (2001) 3016.